https://dx.doi.org/10.1016/j.measurement.2021.108966

Novel Fiber Bragg Grating-based Strain Gauges for Monitoring Dynamic Responses of Celtis Sinensis under Typhoon Conditions

by

Pei-Chen WU
Department of Civil and Environmental Engineering
The Hong Kong Polytechnic University, Hong Kong, China
Email: peichen.wu@connect.polyu.hk

Dao-Yuan TAN (Corresponding Author)
Department of Civil and Environmental Engineering
The Hong Kong Polytechnic University, Hong Kong, China
Email: dao.y.tan@polyu.edu.hk

Wen-Bo CHEN
Department of Civil and Environmental Engineering
The Hong Kong Polytechnic University, Hong Kong, China
Email: geocwb@gmail.com

Numan MALIK
Department of Civil and Environmental Engineering
The Hong Kong Polytechnic University, Hong Kong, China
Email: numan.malik@connect.polyu.hk

Jian-Hua YIN
Department of Civil and Environmental Engineering
The Hong Kong Polytechnic University, Hong Kong, China
Email: cejhyin@polyu.edu.hk

Abstract

In recent decades, conventional electric instruments have been widely adopted to monitor rupture failure of trees by measuring the longitudinal strains of tree trunks. However, the good measurement accuracy is compromised by the significant difference in stiffness of the sensing element and tree trunks. Besides, the reliability of electric instruments under harsh environments, especially extreme weathers, such as thunderstorms and typhoons, is also doubtful. In this study, a novel strain gauge based on fiber Bragg grating (FBG) sensing technology was developed specifically for measuring the strain distribution of tree trunks under static or dynamic loading. The main principle of the design of the strain gauges is presented in detail. The laboratory calibration proves that the FBG-based strain gauges in polyoxymethylene (POM) and polylactic acid (PLA) backings show a better performance than those made of metal. To test the performance of this novel FBG-based strain gauge, a set of transducers were installed at different heights of a *Celtis sinensis*. Firstly, a pull test on this tree trunk was conducted to validate the good performance of the novel strain gauge when the tree is subjected to static loading. Secondly, the good dynamic performance of the novel strain gauge is proved by successfully recording the dynamic motion of a tree trunk during a typhoon. Furthermore, a monitor system relied on the FBG-based strain gauges is conceived to assess the resilience of urban ecosystems formed by trees to extreme weather events.

Keywords: Tree monitoring, strain measurement, optical fiber sensing, typhoon

1. Introduction

The geographical position of Hong Kong makes it susceptible to weather-related threats especially typhoons, like many other tropical and sub-tropical coastal cities. Since records began in 1946, twelve super-typhoons, two in the past three years, have hit Hong Kong. Among those, the super-typhoon (*Mangkhut*) in 2018 was the most severe storm that ever hit Hong Kong over the past 100 years (Abbas *et al*., 2020). Accompanied strong winds and torrential rains have caused disastrous damages to both humans and ecosystems.

Monitoring of trees under wind loads can be of great necessity for evaluating status of trees and protecting trees from failure. The damage of trees caused by wind loads can be divided into stem breakages and root-plate overturning (Marchi *et al*., 2018). Monitoring systems on trees usually rely on strain gauges for measuring the strain (Moore *et al*., 2005), tiltmeters for measuring the stability of root plate (James *et al*., 2013), displacement sensors for measuring the deflection, and accelerometers for measuring the oscillation (Hassinen *et al*., 1998; Rudnicki *et al*., 2001; Rodriguez *et al*., 2012). However, Hassinen *et al*. (1998) also pointed out the accelerometers overestimate the low frequency response of trees under wind loads. It is more popular to directly measure the sway motions or the strain responses of trees. Nicholson (1971) and Muneri *et al*. (1999) designed and used a dial gauge-based instrument to measure the growing strains of trees. Moore *et al*. (2005) invented a strain gauge-based transducer for measuring the dynamic response of trees. Although strain gauges have been widely employed for engineering purposes, the inherent shortages of traditional electrical resistance and vibrating wire strain gauges including malfunction due to electromagnetic interference and unsuitability for long-distance measuring, show the difficulties of the application in harsh environments, such as thunderstorms and typhoons. As optical fiber sensing techniques boost in this century, the drawbacks of conventional sensors based on electronic signals could be overcome by adopting the optical fiber sensors.

Optical fiber sensing based on, such as fiber Bragg grating (FBG) technology, Brillouin optical time-domain analysis (BOTDA) technology, and optical frequency domain reflectometry (OFDR) technology, have been developed and adopted as reliable tools for health monitoring in civil engineering projects (Lima *et al*., 2008; Kerrouche *et al*., 2009; Soto *et al*., 2010; Arsenault *et al*., 2013; Ding et al., 2018; Feng *et al*., 2019). Among different optical fiber sensing techniques, FBG sensing technology has attracted much attention because of its relatively low cost, high accuracy, capacity of multiplexing, and immunity to electromagnetic interference. Therefore, various types of FBG-based transducers have been invented and employed in recent decades (Zhu,2018; Hong *et al*., 2019; Qin *et al*., 2020; Chen *et al.*, 2020; Yin *et al*., 2020). Successful experience of using FBG-based transducers for health monitoring in structures provides an enlightening idea for monitoring trees and forests through similar instruments, such as FBG-based strain gauges. Due to fragility of the fiber itself, FBG fibers are usually attached to or encapsulated in backing materials. Recently, 3-D printing technique has been utilized to fabricate FBG-based transducers with good performance (Leal-Junior *et al*., 2018, 2019 and 2020). Two typical designs of FBG-based strain gauges are shown in Figure 1. Similar designs can be also found in Schulz *et al*. (2001), Zhou *et al*. (2003), Zhu (2009), Schilder *et al*. (2012). However, these transducers might not be feasible to measure the strains of tree trunks whose mechanical properties are not compatible with those of the backing materials of the transducers which are originally designed for concrete or steel structures in civil engineering.

A newly designed FBG-strain gauge for strain measuring on tree trunks is proposed in this study. The principle of the FBG strain gauges and backing materials selection based on a set of calibration tests are described and followed by in-situ calibration on a *Celtis sinensis* (Chinese hackberry tree) by pulling tests. Monitoring results of the responses of trees under strong winds during a recent typhoon are presented and discussed at the end of this paper.

2.Principles and materials

2.1 Principle of the FBG strain gauge transducer

The main principle of the FBG sensor is shown in Figure 2. An incident optical signal with the wavelength of λ passes the Bragg gratings engraved in the fiber reflecting a signal with the Bragg wavelength of λ_B which is determined by Morey *et al*. (1989):

$$\lambda_B = 2 n_{eff} \Lambda \tag{1}$$

where n_{eff} is the effective core refractive index of the optical fiber and Λ is the grating period. Changes in strain ($\Delta\varepsilon$) and temperature (ΔT) induce a Bragg wavelength shift ($\Delta\lambda_B$), which can be represented by (Morey *et al*., 1989; Hill and Meltz, 1997):

$$\frac{\Delta\lambda_B}{\lambda_{B0}} = (1 - p_e)\Delta\varepsilon + (\alpha + \xi)\Delta T = c_\varepsilon \Delta\varepsilon + c_T \Delta T \tag{2}$$

where λ_{B0} is the original Bragg wavelength; p_e is the effective photo-elastic coefficient; α is the thermal expansion coefficient of the fiber material; ξ is the thermo-optic coefficient; c_ε is the coefficient of strain with a typical value of 0.78, and c_T is the coefficient of temperature with a typical value of $6.67 \times 10^{-6} / {}^\circ C$.

Since the temperature in the laboratory is stable at 25℃± 0.2℃, the wavelength shift in FBG sensors due to the temperature change is negligible compared with the wavelength shift caused by strain increments, and hence the strain measured by the FBG sensors is:

$$\varepsilon_{measured} = \frac{\Delta\lambda_B}{c_\varepsilon \lambda_{B0}} + \varepsilon_0 \quad (3)$$

where ε_0 is the initial strain, which is considered as zero for the calibration test.

2.2 Transducer design and installation

The FBG-based strain gauge is fabricated by encapsulating a commercial FBG sensor, whose specifications are listed in Table 1, in a small backing (65 mm-long in total) for supporting and protecting the fragile fiber gratings. The measured strain is the average values of the strains along the length covered by the strain gauge from the center of one end of the small backing to the other end. Different designs of the backing in terms of shape and size were optimized and iterated by 3D-printing technology to reach a perfect shape of the prototype, as shown in Figure 3.

To measure the accurate and reliable strain of the tree trunk, compatibility of backing materials of FBG-based strain gauges to be used for transferring strain from trunk to FBG sensors is a prominent concern. Cannel and Morgan (1987) reported that the Young's modulus of a living tree trunk is around 2.4-7.5 GPa. The transducers designed by Moore *et al*. (2005) to measure the dynamic behavior of trees were made of aluminum with Young's modulus around 70 GPa, which is too stiff compared to tree trunks. It is doubtful whether the significant difference in the moduli of transducers and trees compromises the accuracy of the measured data. Therefore, the main idea of backing design is to use the materials possessing a compatible Young's modulus to that of the living tree trunks or to use thin flexible foils. Generally, engineering plastics have a lower Young's modulus compared to conventional metals and have been widely adopted for medical and sensing applications (Penick *et al*., 2005; Ni *et al*., 2017). Polylactic acid (PLA), polyoxymethylene (POM), and beryllium bronze foil are selected to fabricate the FBG-based strain gauges. The performances of different backings are checked by a set of calibration tests in the laboratory condition. Rakhshtadt *et al*. (1960), Rémond and Védrines (2004), Kamthai and Magaraphan (2015) presented Young's moduli of beryllium bronze foil, POM, and PLA, respectively, as shown in Table 2. In this study, the PLA backings were manufactured by 3D printing, while the other two types of backings were manufactured by computer numerical control (CNC). The FBG-based strain gauges formed by encapsulating FBG sensors with backings using epoxy can be mounted by self-tapping screws on a tree trunk or other testing objects, as shown in Figure 3.

3.Testing methods

The purpose of conducting a laboratory calibration is to select the most suitable backing for field testing and assess the reproducibility and repeatability of the FBG-based strain gauge. The purpose of conducting a field testing is to test the performance of FBG-based strain gauges with selected backing on a Celtis Sinensis tree. The testing methods and setups are described in this Section, while the testing results will be described in Section 4.

3.1 Laboratory calibration

FBG-based strain gauges were mounted on a wood beam with a length of 900 mm and a rectangular cross-section area of 98 mm × 22 mm. One end of the wood beam is fixed, while another end is supported by a precision motion control device on an advanced calibration platform to form a cantilever, as shown in Figure 4. The precision motion control device allows to precisely apply a displacement at a small level of 0.01 mm to the wood beam. Such a configuration provides the wood beam a pure bending condition during the calibration. According to the bending theory of cantilevers, the bending moment at a given point (x) can be expressed as:

$$M = p\left(a - x\right) \tag{3}$$

where a is the distance from the loading point to the fixed end, p is the applied loading at the loading point. The theoretical strain at the given point (x) is:

$$\varepsilon = \frac{\sigma}{E} = \frac{MD/2}{EI} = \frac{p(a-x)D/2}{EI} \tag{4}$$

where D, E, I are the thickness, Young's modulus, and moment of inertia of the wood beam, respectively. Using the beam deflection formulas (Gere and Goodno, 2013), the relationship between the applied loading and corresponding displacement at the loading point ($x = a$) can be expressed as:

$$\Delta y = \frac{pa^2}{6EI}\left(3x - a\right) = \frac{pa^2}{6EI}\left(3 \times a - a\right) = \frac{pa^3}{3EI} \tag{5}$$

Combining Eqs. (4) and (5), the relationship between applied displacement and theoretical strain at the given point (x) is expressed as:

$$\varepsilon = \frac{3\Delta y\left(a - x\right)D}{2a^3} \tag{6}$$

The layout of the FBG-based strain gauges with different backings on the wood beam is illustrated in Figure 4. B1, B2, and B3 are three strain gauges with beryllium bronze backing;

PLA1, PLA2, PLA3, and PLA4 are four strain gauges with 3D-printing PLA backing; POM1 and POM2 are two strain gauges with POM backing. The purpose of installing duplicated strain gauges is to check the reproducibility. The original point of the axis is set at the fixed end of the wood beam, and the loading point is located at 850 mm. For each loading test, at least two loops (loading-unloading) were conducted to ensure the repeatability.

Meanwhile, the optical frequency domain reflectometry (OFDR) sensing technology (optical fibers and an OFDR interrogator) with a spatial resolution of 10 mm was also used to measure the strain responses along the wood beam under different displacements. The sensing fiber for OFDR using was attached on the wood beam from 0.12 m to 0.85 m, represented by the effective measurement range. The fiber beyond this range did not attach to the wood beam and only worked as a jumping cable to transmit optical signals, as shown in Figure 5. The OFDR technology has been successfully used for strain measurement in civil, mechanical, and aerospace applications, even for flexible structures (Henault *et al*., 2011; Lally *et al*., 2012).

3.2 Field testing

Based on the analysis and results determined from the laboratory calibration tests, which will be described in Section 4, the FBG-based strain gauges with POM backing are selected for field testing. A *Celtis sinensis* (Chinese hackberry tree) with the height of its main trunk of 4.3 m, diameter at breast height of 33 cm, was equipped with FBG-based strain gauges at different heights and chosen for conducting a pulling test. Figure 6 illustrates the testing process, applied displacements, and layout of the FBG-based strain gauges. The FBG-based strain gauges were installed at the heights of 3.95 m and 2.92 m on the tree trunk using the identical method as that adopted for laboratory calibration tests. A fiber for OFDR was also attached to the tree from 1 m to 4.3 m and connected to the OFDR interrogator. The strain responses of the tree trunk recorded by the OFDR interrogator during the fielding testing are regarded as the reference to check the in-situ responses of the FBG-based strain gauges.

The pulling system used for field testing consists of a steel strand cable, a cable puller, and a laser distance meter. One end of the steel strand cable is tied on the top of the main trunk where the main tree trunk starts to bifurcate into two branches, while the other end is tied on the steel frame attached to a concrete block. During the pulling test, staged displacements were applied on the top of the main trunk and measured by the laser distance meter. The sampling rate for FBG-based strain gauges was set as 10 Hz, which is capable of covering the sway frequencies (up to 2Hz) of trees (James *et al*., 2006). For the strain measurement using OFDR technology, the strain distribution along the tree trunk was scanned and recorded when the tree reaches a stable position after each staged displacement.

4.Results and discussion

4.1 Laboratory calibration results

The calibration results of FBG-based strain gauges with different backings are shown in Figure 7. The slope of the correlation lines represents the relationship between the theoretical strain and measured strain. The ideal unit slope indicates that measured strain equals theoretical strain, as shown by the dashed lines. If the value of the slope is larger than one, the measured strain underestimates the theoretical strain. Otherwise, the measured strain overestimates the theoretical strain. The calibration results on the strain gauges with beryllium bronze backing (B1, B2, and B3) show the value of the slope in a range from 1.41 to 2.45, revealing that the beryllium bronze foil is not a good backing material to transfer the strain of wood beam to FBG sensors. The calibration results on the FBG-based strain gauges with PLA backing (PLA1, PLA2, PLA3, and PLA4) show the value of the slope in a range from 0.85 to 1.13, which are quite close to unit, indicating that the PLA backing is capable of deforming compatibly with the wood beam. The calibration results on the strain gauges made of POM backing (POM1 and POM2) give the slopes with the values of 0.93 and 1.19, proving that POM backing is also able to have a consistent strain response as that of the wood beam.

A further correlation analysis is carried out between the ideal line of $y = x$ and the data from the calibration tests, with the values of correlation coefficient listed in Table 1. The strain of the wood beam can be well transferred to the FBG sensors bridging by both POM and PLA backings under the current configuration and mounting method. However, PLA has a glass transition temperature of around 55℃ (Szycher, 1991). It is highly likely to exceed this temperature under summer sunlight, which may cause significant changes in its mechanical properties. In contrast, the glass transition temperature of POM is around -60℃, which is beyond the range of working temperature of the FBG sensors. Given other advantages such as high strength, hardness, and rigidity, the POM backings are selected as the backing mechanism for FBG-based strain gauges for tree monitoring. Besides, a *t*-test is also carried out on the theoretical strains caused by applied displacement and the strains measured by FBG-based strain gauges made of POM, indicating that the strain caused by the applied displacement accounts for 99.6% of the variation in the output of the FBG-based strain gauges made of POM. Therefore, the FBG-based strain gauges with POM backing are selected for field testing.

Figure 5 shows the good consistency of the strain measurement conducted in the laboratory using OFDR technology on a wood beam. However, considering that data scanning and processing by the OFDR interrogator is time-consuming (depending on the measured length. 3 s was needed in this study), this method is not suitable for measuring dynamic strain but can be used in pulling tests in which the strain responses can be considered as static. Therefore, the OFDR technology is also applied in field testing to provide a reference measurement for FBG-based strain gauges with POM backing.

4.2 Field testing results

Figure 8 presents the strain profiles along the tree trunk measured by OFDR and the strain measured by the FBG-based strain gauges at different heights. Due to the irregular cross-section of the tree, the strain profiles of the tree trunk are not as linear as those of a simple cantilever beam. Nevertheless, the trend of that strain along the tree trunk increases with the decrease in the height, which agrees well with that of a cantilever beam subjected to a point loading. The sudden increase in strain over 4.3 m is due to the stress concentration caused by the steel strand which was tied on the top of the tree trunk. Figure 9 shows the relationship between the strains measured by the FBG-based strain gauges at the heights of 2.92 m and 3.95 m and the reference strains measured by OFDR at the same locations. The fitting line is formulated by a linear function with a high correlation coefficient at the location of each FBG-based strain gauge. The slope of the fitting lines represents the difference between the strain measured by FBG-based strain gauges and that measured by OFDR. At 3.95 m height, the slope of the fitting line is 1.051 indicating good consistency between the strains measured by FBG-based strain gauges and OFDR technology. At 2.92 m height, the slope increases to 1.257 indicating that the FBG-based strain gauges slightly underestimate the strain at a lower height. Overall, considering the heterogeneity in geometry and mechanical properties of living trees, the new FBG-based strain gauge has a good performance in measuring the strains of trees the difference between these two measurements is acceptable.

The results of the field test validate that the developed strain gauges can accurately reflect the strains on a tree.

5.Responses of the FBG-based strain gauge under strong winds

The typhoon season occurs in Southeast Asia every year from June to September. There was a reported Typhoon (*Higos*) that affected Hong Kong from 18 August 2020 to 19 August 2020 (Hong Kong Observatory, 2020). The strain responses at different heights of the monitored tree under this typhoon were recorded by the FBG-based strain gauges, as shown in Figure 10. It is found that the strain at 3.95 m height is lower than that at 2.92 m of the tree trunk. This is probably due to damping effect of the canopy of the tree which mitigates the sway at the top of the tree trunk, and thus reduces the strain. The maximum strain responses at different heights of the tree trunk occurred at 03:30 AM of 19 August 2020, which agrees well with the intensity of Typhoon *Higos* recorded by Hong Kong Observatory.

Figure 11 shows the spectral analysis of the strains showed a constant broad peak at 0.46 Hz at different heights, with some other closely spaced sway frequencies present. This is consistent with the dynamic response of a tree with large side branches, that prevent any large oscillations with dangerous harmonic sways (James *et al*., 2006). The oscillation frequency obtained from the FBG-based strain gauges is within the frequency range of 0.3-1.5 Hz, reported by Baker (1997) and James *et al*. (2006) measured by laser beams and conventional electronic strain gauges.

Based on the successful experience from the strain measurement under typhoon loading, a smart monitoring system can be set up using the FBG-based strain gauges to study the dynamic behavior of trees under extreme weathers and capture dangerous situations of the monitored trees for preventing damages of the trees or injuries of people nearby. Considering that the wavelength shifts of the FBG sensors are also related to temperature change, for long-term monitoring with significant temperature fluctuations, additional FBG-based transducers with a cantilever-like backing, which only experience the temperature effects can be installed adjacent to the FBG-based strain gauges for temperature measurement and compensation as shown in Figure 12.

6.Conclusion

Based on FBG sensing technology, a novel strain gauge for tree monitoring is designed and tested in both laboratory and in-situ conditions. Laboratory calibration tests verify that POM and PLA backings with similar Young's moduli to that of living tree trunks deform compatibly with the wood beam. It is confirmed from the measured data of the strain gauges with beryllium bronze backings that the significant difference in the moduli of transducers and trees does reduce the accuracy of the strain measurement. Considering the thermostability of the backings under working temperature and good mechanical properties, the FBG-based strain gauges with POM backings are recommended. An in-situ pulling test was conducted on a *Celtis sinensis* to demonstrate the reliability of the strain measurement of the FBG-based strain gauges. The responses of the monitored tree under typhoon loading were well captured by the FBG-based strain gauges and showed a good agreement with the intensity of the typhoon recorded by the Hong Kong Observatory. Besides, using the proposed strain gauges, the oscillation frequency of the *Celtis sinensis* which is 0.46 Hz was measured under typhoon conditions. Compared with existing transducers, the main improvements of the new FBG-based strain gauges proposed in this study are listed in Table 3.

Acknowledgement

The work in this paper is supported by the Development Bureau of Hong Kong SAR Government, a Research Impact Fund (RIF) project (R5037-18), a Theme-based Research Scheme Fund (TRS) project (T22-502/18-R), and three General Research Fund (GRF) projects (PolyU 152209/17E; PolyU 152179/18E; PolyU 152130/19E;) from Research Grants Council (RGC) of Hong Kong SAR. The authors also acknowledge the financial supports from Research Institute for Sustainable Urban Development of The Hong Kong Polytechnic University and three grants (BBAG, ZDBS, ZVNC) from The Hong Kong Polytechnic University.

References

Abbas, S., Nichol, J. E., Fischer, G. A., Wong, M. S., & Irteza, S. M. (2020). Impact assessment of a super-typhoon on Hong Kong's secondary vegetation and recommendations for restoration of resilience in the forest succession. Agricultural and Forest Meteorology, 280, 107784.

Arsenault, T. J., Achuthan, A., Marzocca, P., Grappasonni, C., & Coppotelli, G. (2013). Development of a FBG based distributed strain sensor system for wind turbine structural health monitoring. Smart Materials and Structures, 22(7), 075027.

Cannell, M. G. R., & Morgan, J. (1987). Young's modulus of sections of living branches and tree trunks. Tree Physiology, 3(4), 355-364.

Chen, W. B., Feng, W. Q., Yin, J. H., & Qin, J. Q. (2020). New FBG-based device for measuring small and large radial strains in triaxial apparatus. Canadian Geotechnical Journal, https://doi.org/10.1139/cgj-2020-0145.

Ding, Z., Wang, C., Liu, K., Jiang, J., Yang, D., Pan, G., ... & Liu, T. (2018). Distributed optical fiber sensors based on optical frequency domain reflectometry: A review. Sensors, 18(4), 1072.

Feng, W. Q., Yin, J. H., Borana, L., Qin, J. Q., Wu, P. C., & Yang, J. L. (2019). A network theory for BOTDA measurement of deformations of geotechnical structures and error analysis. Measurement, 146, 618-627.

Gardiner, B. A. (1995). The interactions of wind and tree movement in forest canopies. Wind and Trees, 41-59.

Gere, J. M., and Goodno, B. J. (2013). Mechanics of Materials. Cengage Learning, Stamford, CT.

Hassinen, A., Lemettinen, M., Peltola, H., Kellomäki, S., & Gardiner, B. (1998). A prism-based system for monitoring the swaying of trees under wind loading. Agricultural and Forest Meteorology, 90(3), 187-194.

Henault, J. M., Salin, J., Moreau, G., Delepine-Lesoille, S., Bertand, J., Taillade, F., ... & Benzarti, K. (2011). Monitoring of concrete structures using OFDR technique. American Institute of Physics Conference Proceedings, 1335(1), 1386-1393

Hill, K. O., & Meltz, G. (1997). Fiber Bragg grating technology fundamentals and overview. Journal of Lightwave Technology, 15(8), 1263-1276.

Hong, C., Zhang, Y., Lu, Z., & Yin, Z. (2019). A FBG tilt sensor fabricated using 3D printing technique for monitoring ground movement. IEEE Sensors Journal, 19(15), 6392-6399.

Hong Kong Observatory. (2020). Tropical Cyclone Warning Signals Retrieved from https://www.weather.gov.hk/en/wxinfo/climat/warndb/warndb1.shtml?opt=1&sgnl=1.or.higher&start_ym=202008&end_ym=202009&submit=Submit+Query

James, K. R., Haritos, N., & Ades, P. K. (2006). Mechanical stability of trees under dynamic loads. American Journal of Botany, 93(10), 1522-1530.

James, K. R., & Kane, B. (2008). Precision digital instruments to measure dynamic wind loads on trees during storms. Agricultural and Forest Meteorology, 148(6-7), 1055-1061.

James, K., Hallam, C., & Spencer, C. (2013). Tree stability in winds: Measurements of root plate tilt. Biosystems Engineering, 115(3), 324-331.

Kamthai, S., & Magaraphan, R. (2015, May). Thermal and mechanical properties of polylactic acid (PLA) and bagasse carboxymethyl cellulose (CMCB) composite by adding isosorbide diesters. American Institute of Physics Conference Proceedings, 1664(1), 060006.

Kerrouche, A., Boyle, W. J. O., Sun, T., & Grattan, K. T. V. (2009). Design and in-the-field performance evaluation of compact FBG sensor system for structural health monitoring applications. Sensors and Actuators A: Physical, 151(2), 107-112.

Lally, E. M., Reaves, M., Horrell, E., Klute, S., & Froggatt, M. E. (2012). Fiber optic shape sensing for monitoring of flexible structures. In Sensors and Smart Structures Technologies for Civil, Mechanical, and Aerospace Systems, 8345, 1-9.

Leal-Junior, A. G., Marques, C., Ribeiro, M. R., Pontes, M. J., & Frizera, A. (2018). FBG-embedded 3-D printed ABS sensing pads: The impact of infill density on sensitivity and dynamic range in force sensors. IEEE Sensors Journal, 18(20), 8381-8388.

Leal-Junior, A. G., Díaz, C., Marques, C., Frizera, A., & Pontes, M. J. (2019). 3D-printing techniques on the development of multiparameter sensors using one FBG. IEEE Sensors Journal, 19(16), 3514.

Leal-Junior, A. G., Rocha, H. R., Theodosiou, A., Frizera, A., Marques, C., Kalli, K., & Ribeiro, M. R. (2020). Optimizing linearity and sensitivity of 3D-printed diaphragms with chirped FBGs in CYTOP fibers. IEEE Access, 8, 31983-31991.

Lima, H. F., da Silva Vicente, R., Nogueira, R. N., Abe, I., de Brito Andre, P. S., Fernandes, C., & de Lemos Pinto, J. (2008). Structural health monitoring of the church of Santa Casa da Misericórdia of Aveiro using FBG sensors. IEEE Sensors Journal, 8(7), 1236-1242.

Livesley, S. J., McPherson, E. G., & Calfapietra, C. (2016). The urban forest and ecosystem services: impacts on urban water, heat, and pollution cycles at the tree, street, and city scale. Journal of Environmental Quality, 45(1), 119-124.

Marchi, L., Grigolato, S., Mologni, O., Scotta, R., Cavalli, R., & Montecchio, L. (2018). State of the Art on the Use of Trees as Supports and Anchors in Forest Operations. Forests, 9(8), 467.

Moore, J. R., Gardiner, B. A., Blackburn, G. R., Brickman, A., & Maguire, D. A. (2005). An inexpensive instrument to measure the dynamic response of standing trees to wind loading. Agricultural and Forest Meteorology, 132(1-2), 78-83.

Morey, W. W., Meltz, G., & Glenn, W. H. (1990). Fiber optic Bragg grating sensors. In Fiber Optic and Laser Sensors VII, 1169, 98-107.

Nicholson, J. E. (1971). A rapid method for estimating longitudinal growth stresses in logs. Wood Science and Technology, 5(1), 40-48.

Ni, Y., Ji, R., Long, K., Bu, T., Chen, K., & Zhuang, S. (2017). A review of 3D-printed sensors. Applied Spectroscopy Reviews, 52(7), 623-652.

Penick, K. J., Solchaga, L. A., Berilla, J. A., & Welter, J. F. (2005). Performance of polyoxymethylene plastic (POM) as a component of a tissue engineering bioreactor. Journal of Biomedical Materials Research Part A: An Official Journal of The Society for Biomaterials, The Japanese Society for Biomaterials, and The Australian Society for Biomaterials and the Korean Society for Biomaterials, 75(1), 168-174.

Qin, J. Q., Feng, W. Q., Wu, P. C., & Yin, J. H. (2020). Fabrication and performance evaluation of a novel FBG-based effective stress cell for directly measuring effective stress in saturated soils. Measurement, 155, 107491.

Rémond, Y., & Védrines, M. (2004). Measurement of local elastic properties of injection moulded polymer structures by analysis of flexural resonant frequencies. Applications in POM, PA66, filled PA 66. Polymer Testing, 23(3), 267-274.

Rodriguez, M., Ploquin, S., Moulia, B., & de Langre, E. (2012). The multimodal dynamics of a walnut tree: experiments and models. Journal of Applied Mechanics, 79(4).

Rudnicki, M., Silins, U., Lieffers, V. J., & Josi, G. (2001). Measure of simultaneous tree sways and estimation of crown interactions among a group of trees. Trees, 15(2), 83-90.

Schilder C., Kohlhoff H., Hofmann D., & Habel W. (2012). Structure-integrated fibre-optic strain wave sensor for pile testing and monitoring of reinforced concrete piles, Proceedings of the 6th European Workshop on Structural Health Monitoring.

Schulz W.L., Conte J.P., & Udd E., (2001). Long-gage fiber optic Bragg grating strain sensors to monitor civil structures, Proceedings of the International Society of Optical Engineering, 4330, 56-65.

Soto, M. A., Bolognini, G., Di Pasquale, F., & Thévenaz, L. (2010). Simplex-coded BOTDA fiber sensor with 1 m spatial resolution over a 50 km range. Optics Letters, 35(2), 259-261.

Szycher, M. (1991). High performance biomaterials: a complete guide to medical and pharmceutical applications. CRC Press.

Yin, J. H., Qin, J. Q., & Feng, W. Q. (2020). Novel FBG-based effective stress cell for direct measurement of effective stress in saturated soil. International Journal of Geomechanics, 20(8), 04020107.

Zhou Z., Graver T. W., Hsu L., & Ou J. P. (2003). Techniques of advanced FBG sensors: fabrication, demodulation, encapsulation, and their application in the structural health monitoring of bridges, Pacific Science Review, 5, 116–121.

Zhu, H. H. (2009). Optical fiber monitoring and performance evaluation of geotechnical structures, (Doctoral dissertation, The Hong Kong Polytechnic University).

Rakhshtadt, A. G., Rogel'Berg, I. L., Vorob'Eva, L. P., & Puchkov, B. I. (1960). The effect of heat treatment on the properties and structure of beryllium bronze. Metal Science and Heat Treatment of Metals, 2(2), 87-98.

Zhu, X. B. (2018). A novel FBG velocimeter with wind speed and temperature synchronous measurement. Optoelectronics Letters, 14(4), 276-279.

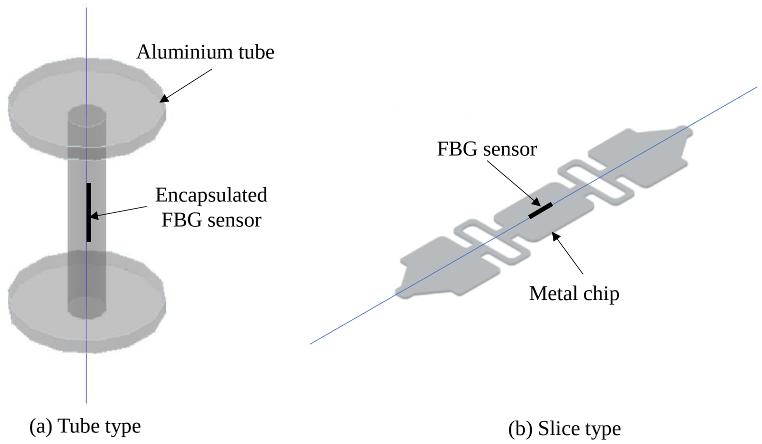

Figure 1. Typical designs of FBG-based strain gauges: (a) tube type (after Zhu, 2009) and (b) slice type (e.g. OS3100 from Micron Optics Inc)

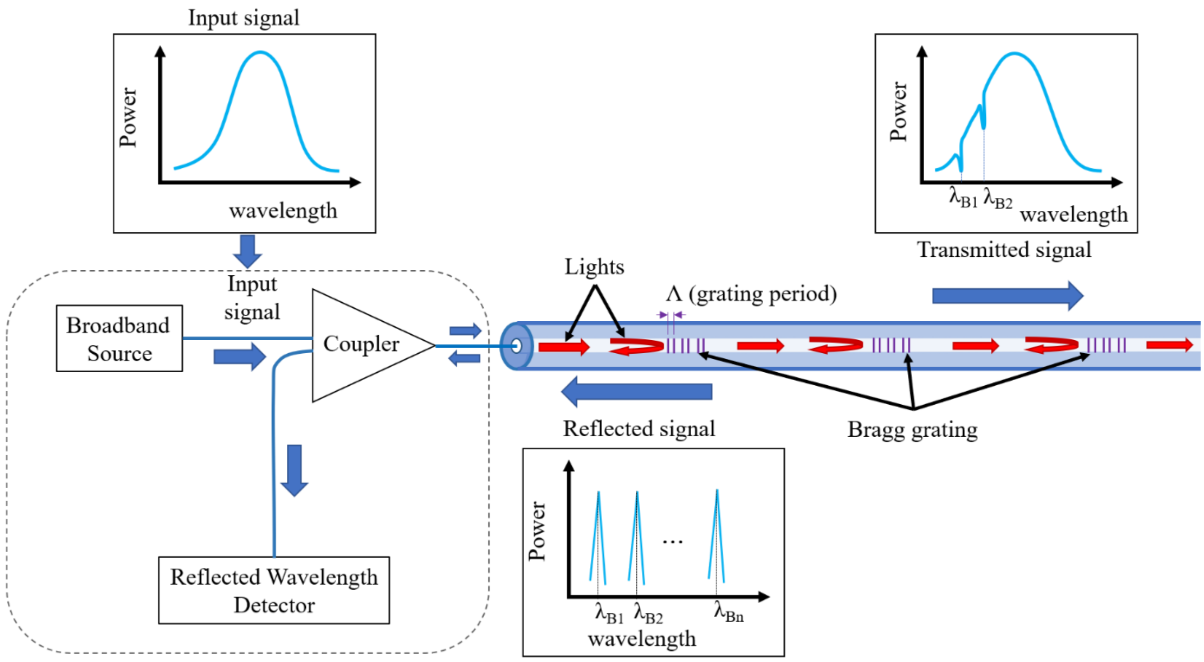

Figure 2. Illustration of the principle of FBG sensing

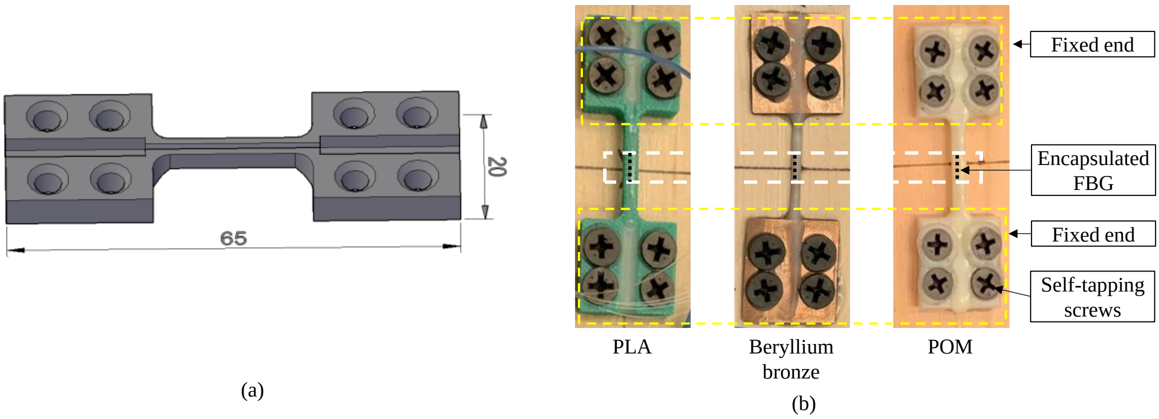

Figure 3. (a) Prototype design of FBG-based strain gauges (unit in mm) and (b) FBG-based strain gauges with different backing materials

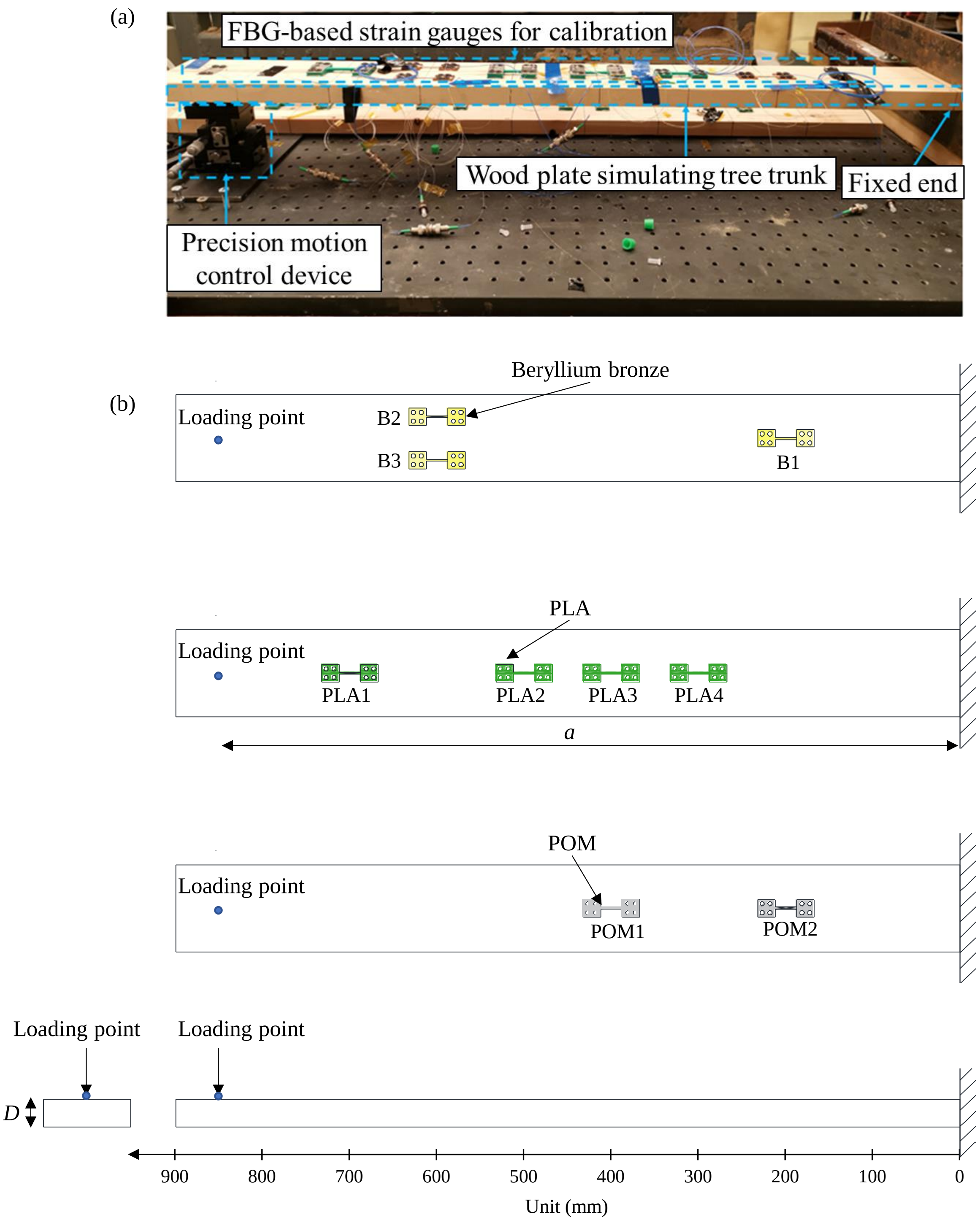

Figure 4. (a) Setup of calibration test and (b) Layout of FBG-based strain gauges with different backing materials on a wood beam

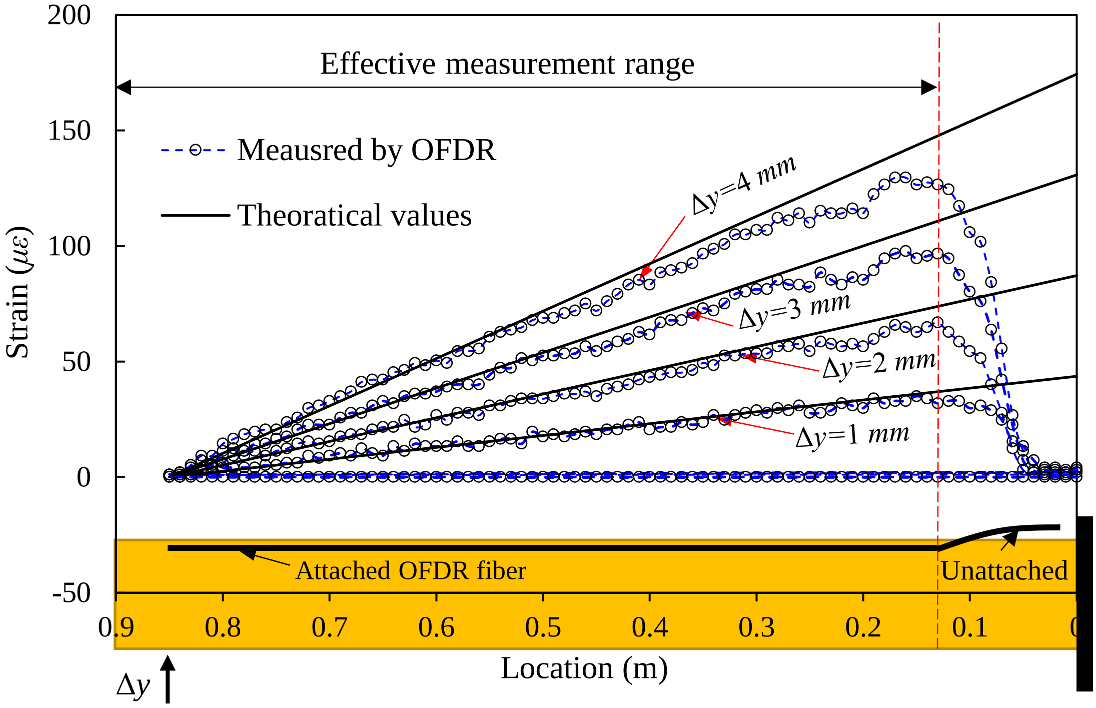

Figure 5. Calibration results of OFDR using a cantilever wood beam

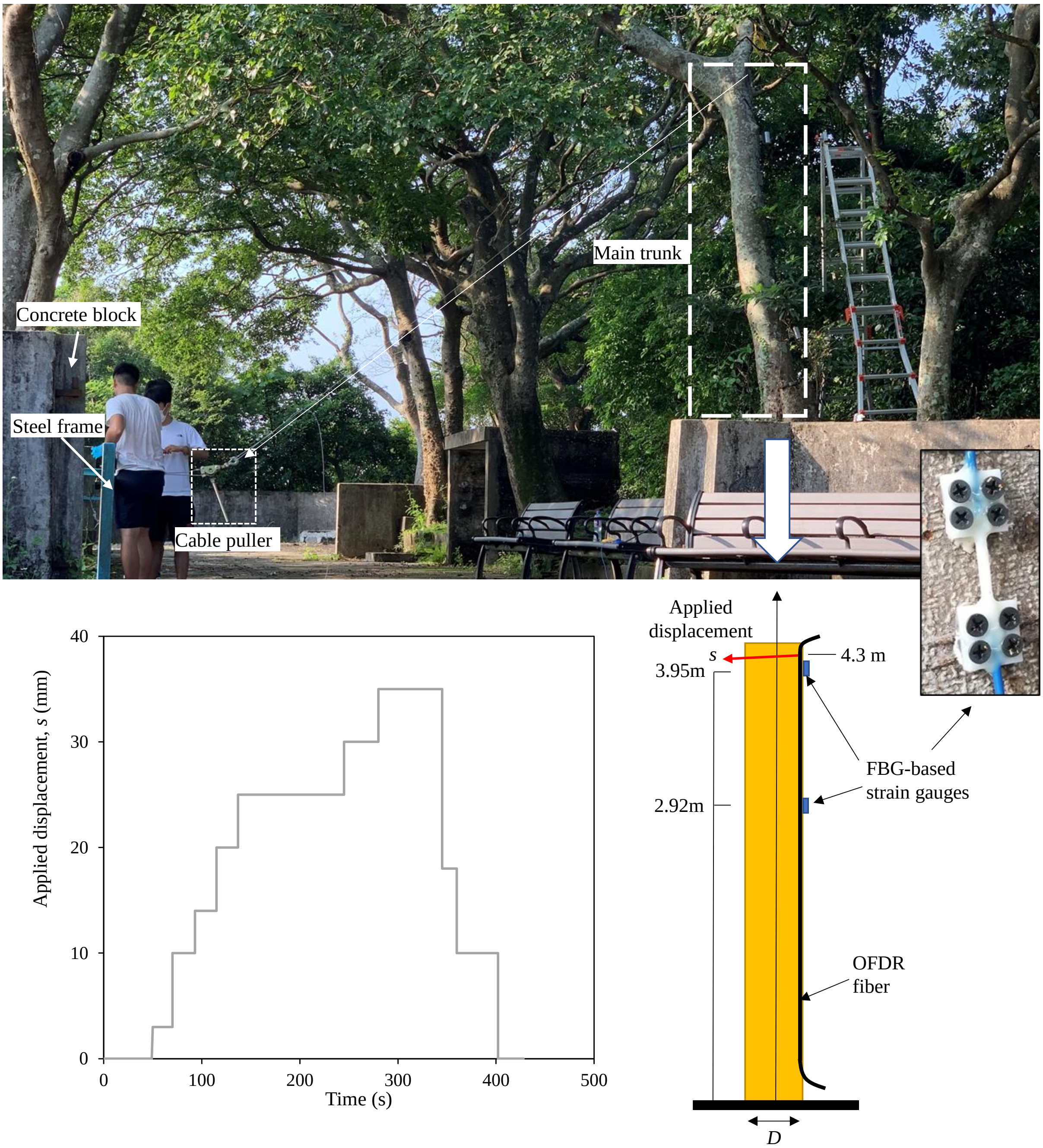

Figure 6. Illustration of in-situ pulling test with its loading schedule and the layout of FBG-based strain gauges

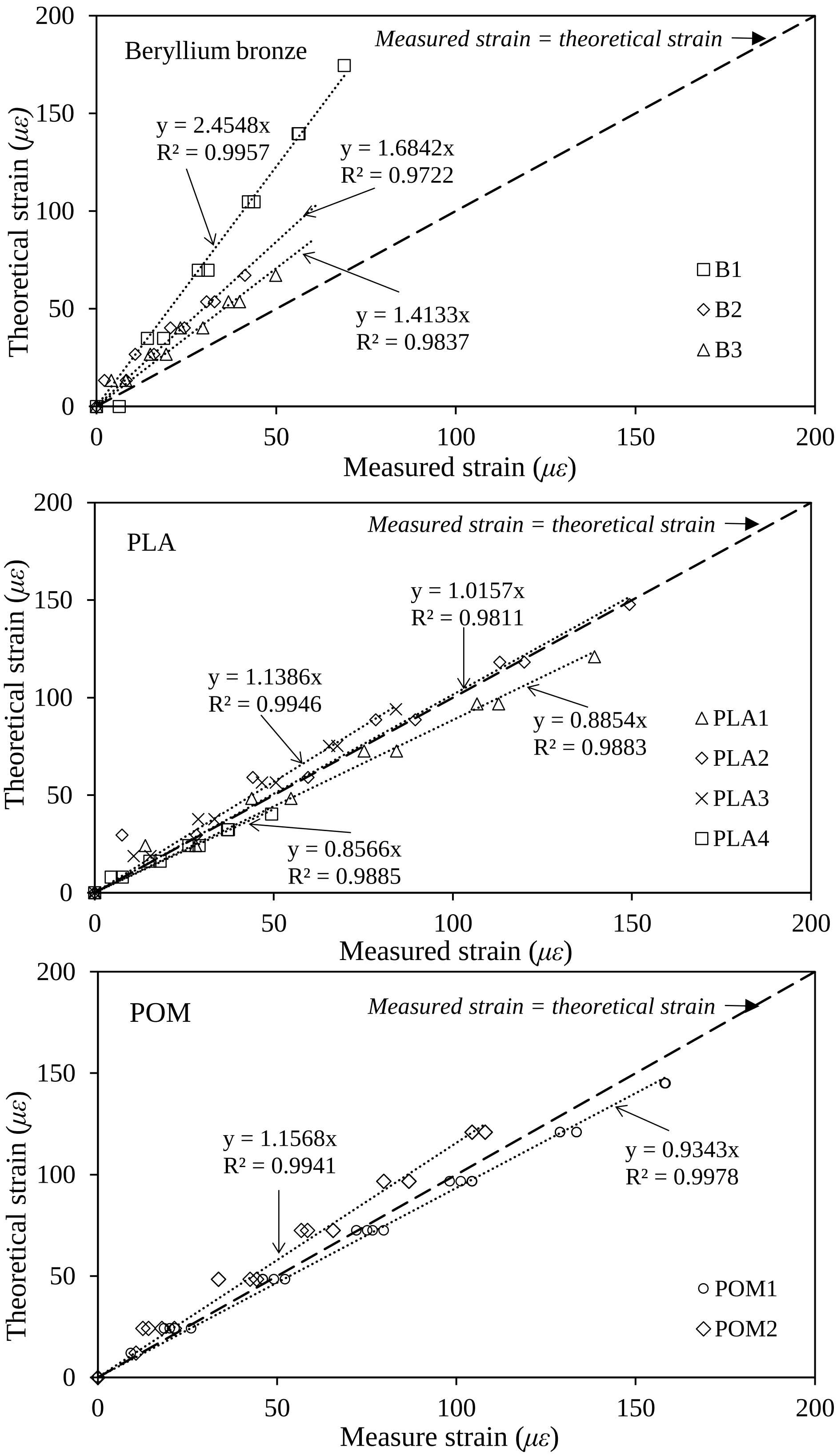

Figure 7. Calibration results on FBG-based strain gauge made by different backing materials

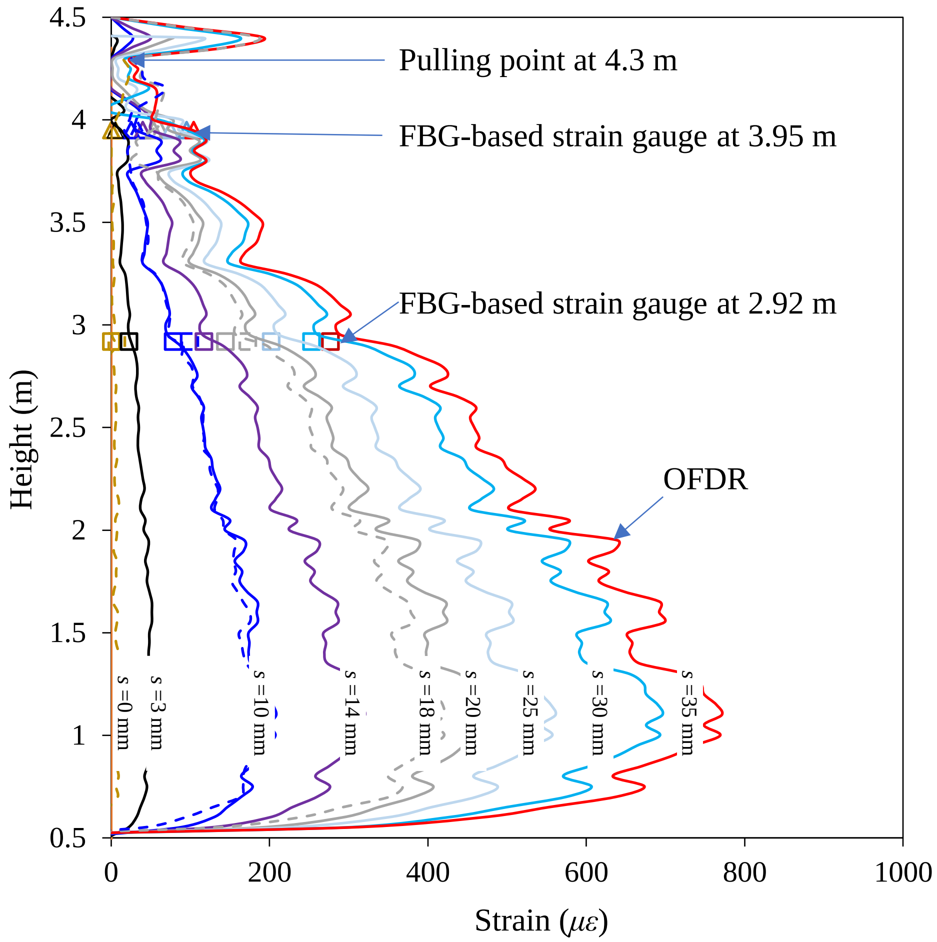

Figure 8. Measured strains by FBG strain gauges and OFDR technology

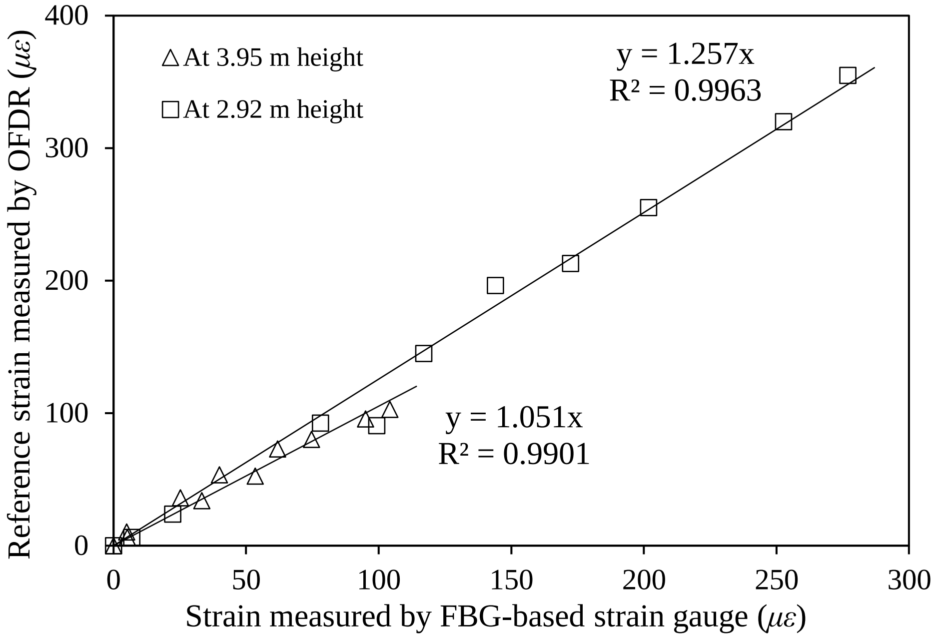

Figure 9. Correlation between the strains measured by FBG-based strain gauges and reference strain measured by OFDR

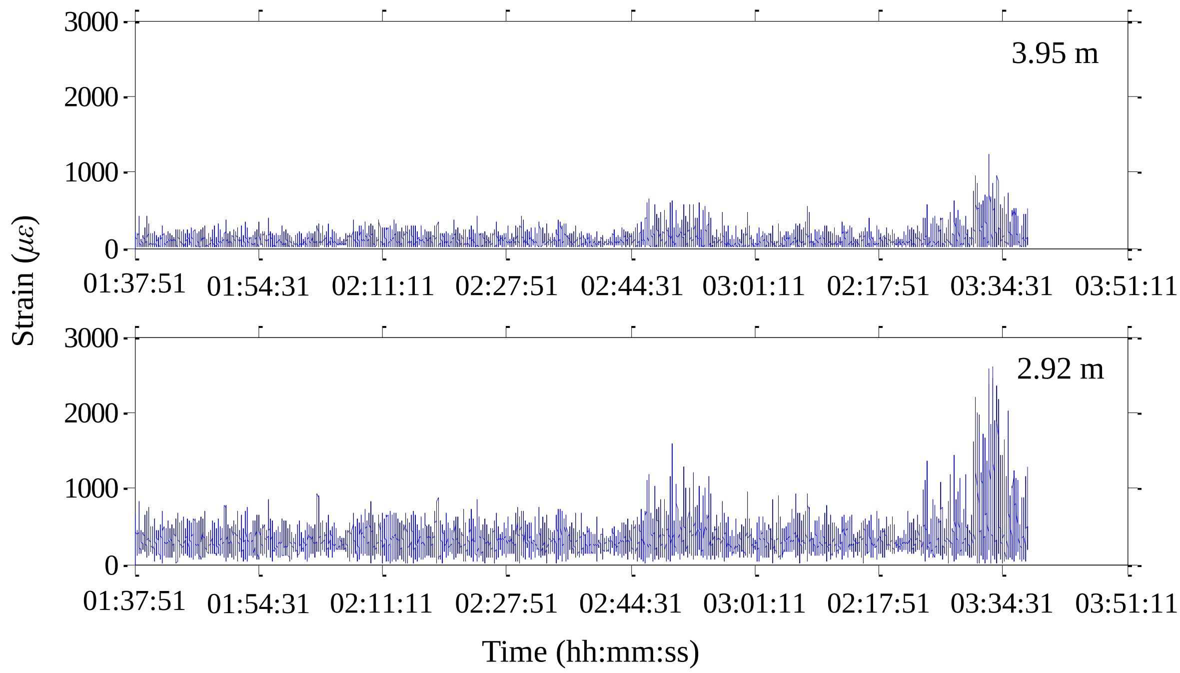

Figure 10. Strain responses of the tree measured by FBG-based strain gauges under strong winds

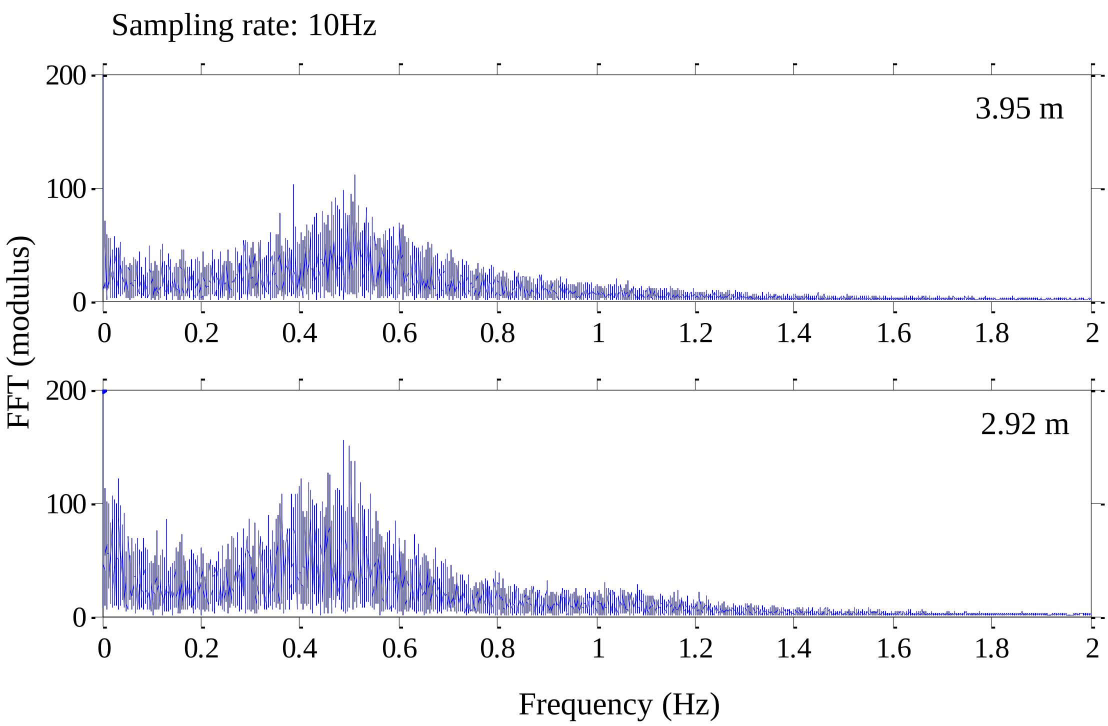

Figure 11. Spectral analysis of the measured data under strong winds

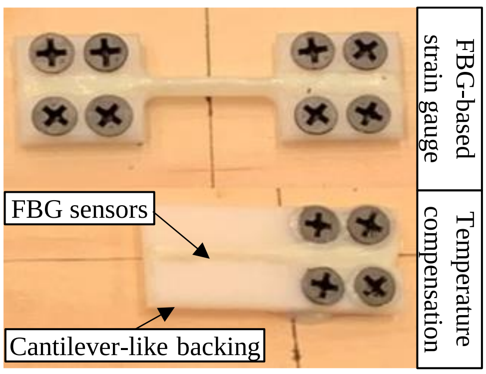

Figure 12. A temperature compensation method

Table 1 Specifications of the FBG sensors

Item	Specification
Center wavelength	1530~1560 nm
FBG length	10 mm
Reflectivity	≥90%
Bandwidth at 3dB	≤0.3nm
Recoating	Acrylate
Fiber type	SMF-28e

Table 2 Description and performance of different backing materials

Material	Description	E (GPa)	R^2
POM	A plastic material with high strength, hardness, and rigidity	3	0.9533
PLA	A plastic material which is commonly used for 3D printing	2	0.9437
Beryllium bronze	Metal with excellent resistance to fatigue and abrasion and ability in elastic recovery	125	0.3371

E is the Young’s modulus, R^2 is the correlation coefficient obtained from the laboratory calibration tests.

Table 3 Comparative study of existing measurement methods for trees movement under wind loads

Method	Principle	Justification
Calliper type strain gauge transducers (Moore et al., 2005)	Electrical conductance	Accuracy is influenced by the significant difference in stiffness between the metal backing materials and living trees; malfunction due to electromagnetic interference and unsuitability for long-distance measuring
Prism-based monitor system (Hassinen et al., 1997)	Measuring displacement by optical signal using prism system	High accuracy for static or dynamic measurement under low winds. Not suitable for typhoon conditions
Indirect measurement using accelerometers (Gardiner, 1995; Hassinen et al., 1997)	Integrating to obtain strain/displacement	Low accuracy due to the accumulated errors caused by integration
Strainmeters (James and Kane, 2008)	Measuring strain by a digital probe	Digital output. Only suitable for those trees with large sized branches because the instrument is 0.5 m long
FBG-based strain gauge in this study	FBG sensing technology	Mini size (65 mm in length), high accuracy, capacity of multiplexing, and immunity to electromagnetic interference, suitable for the measurement under extreme weathers such as typhoons